BLIND AND AFTERMATH NUMERICAL ANALYSES OF SUPERCRITICAL WATER FLOW AND HEAT TRANSFER IN 1/12 OF 7-ROD BUNDLE WITH SPACERS

P. Műhlbauer, O. Frýbort, and K. Gregor*
Research Centre Rez Ltd.
Husinec – Řež 130
CZ 250 68
Czech Republic
Petr.Muhlbauer@cvrez.cz; Otakar.Frybort@cvrez.cz; Karel.Gregor@cvrez.cz

ABSTRACT

Application of supercritical water to conventional power plants has provided nuclear community with some experience which can be used in development of future generation of nuclear power plants. Nevertheless there are some specific features of nuclear power plants which should be studied during preparations of pilot designs. In 2013, the Gen-IV International Forum initiated a numerical benchmark based on experimental data obtained in a 7-rod bundle with spacers. It was a "blind" benchmark; the experimental data from a supercritical water test facility at Japan Atomic Energy Agency (JAEA) were revealed to participants during a meeting in June 25-26, 2014 at Delft.

This paper deals with numerical results, obtained at Research Centre Rez during the "blind" phase of the benchmark and also results of some aftermath computations. Main goal was to test ability of the ANSYS FLUENT 12 code to simulate supercritical water flow and heat transfer in rod bundles using moderate-size computational grids.

In order to limit the range of involved parameters, only one model of turbulence (SST k-ω) was selected; physical properties of supercritical water were calculated by REPROP 7 package. Mainly the results for Case B2 where water temperature crosses the pseudo critical temperature are presented here. Several computational grids with increasing size were produced with GAMBIT 2.4.6 preprocessor, and skewness, aspect ratio and size change were selected as monitored characteristics of grid quality. Due to hardware limitations, only 1/12 of the bundle was modeled. In all blind calculations, heat transfer deterioration region appeared when case B2 was simulated. The main results (wall temperatures) obtained using all grids were compared with measured data. Aftermath simulations were focused on determination of effects of buoyancy and spacers on heat transfer phenomena.

KEYWORDS
Supercritical water, CFD, benchmark, computational grid

NOMENCLATURE

CFD	Computational Fluid Dynamics
HTD	Heat Transfer Deterioration
JAEA	Japan Atomic Energy Agency
T_{PC}	Pseudo-critical Temperature

* Corresponding author

1. INTRODUCTION

Numerical simulations of supercritical water flow and heat transfer in channels became more important when nuclear reactors with water at supercritical pressure were selected as an option of future nuclear power plants. Prevailing number of such simulation is still related to circular tubes, but increasing number of experiments on rod bundles modeling nuclear reactor fuel assemblies leads to attempts to simulate supercritical water flow and heat transfer in such complex domains.

In 2013, the Gen-IV International Forum initiated a numerical benchmark based on experimental data obtained in a 7-rod bundle with spacers. It was a "blind" benchmark; the experimental data (3 cases) from a supercritical water test facility at Japan Atomic Energy Agency (JAEA) were revealed to participants during a meeting in June 25-26, 2014 at Delft.

The "blind" benchmarks in fact simulate very frequent situation of an analyst when he is faced with a problem for which there is only limited information. He then must select right "tools" for tackling the problem and use these tools properly. It is a good practice to follow recommendations in textbooks on numerical methods and computational fluid dynamics which includes also performance of validation computations.

This paper deals with numerical results, obtained at Research Centre Rez during the "blind" phase of the benchmark and also results of some aftermath computations. Main goal was to test ability of the ANSYS FLUENT 12 code to simulate supercritical water flow and heat transfer in rod bundles using moderate-size computational grids.

In order to limit the range of involved parameters, only one model of turbulence (SST k-ω) was selected on the basis of our validation calculations of experiment with supercritical water flow in vertical circular tube [2]. This model of turbulence was recommended also by other authors, see e.g. [3]. Physical properties of supercritical water dependent on temperature were calculated by REPROP 7 package which is incorporated in the ANSYS FLUENT 12 code. Mainly the results for Case B2 where water temperature crosses the pseudo critical temperature T_{PC} are presented here. Four computational grids with increasing size were produced with GAMBIT 2.4.6 preprocessor, and skewness, aspect ratio and size change were selected as monitored characteristics of grid quality. Due to hardware limitations, only 1/12 of the bundle was modeled. It is clear that not all possible circumstances of experiment like probable rod bowing can be simulated with this assumption.

In all blind calculations, heat transfer deterioration region appeared when case B2 was simulated. The main results (wall temperatures) obtained on all grids were compared with measured data. Aftermath simulations were focused on determination of effects of buoyancy and spacers on heat transfer phenomena.

2. SIMULATED EXPERIMENTAL CASES

Detailed data on experimental facility at Japan Atomic Energy Agency (vertical bundle of 7 rods) and measured cases can be found in [1]. Pressure drop and outer wall temperature on 7 rods (one central, designated here A and six peripheral, designated B, C, D, E, F and G) with heated length of 1.5 m, outer rod diameter of 8 mm, inner cladding diameter of 6 mm and rod pitch of 9 mm were measured by thermocouples at selected rods, axial levels, and azimuthal angles.

Three measured cases were included in the benchmark as shown in Table I provided by JAEA experimentalists. The first, Case A1, is a constant-temperature case (no heat flux on cladding surfaces)

where pressure drop between axial levels 0.144 m and 1.340 m was measured. In the Case B1, water temperature remains under the pseudo-critical temperature T_{PC} whereas in the Case B2, the pseudo-critical temperature is crossed with consequent large changes of water physical properties.

Table I. Data on the simulated cases as provided by the JAEA

Case	Inlet temperature [K]	Inlet pressure [MPa]	Flow rate [kg/s]	Heater A [kW]	Heater B, D, F [kW]	Heater C, E, G [kW]
Case A1	297.6	25.0	0.4389	-	-	-
Case B1	353.6	24.98	0.2815	19.67	22.51	22.52
Case B2	519.6	25.03	0.2753	34.14	34.08	34.13

3. NUMERICAL PROCEDURE

It was decided, that during the blind phase, a set of computational meshes with systematically increased number of cells (mesh density) will be used keeping in mind hardware limitations. The following assumptions were also adopted:

- Only 1/12 of the bundle was simulated (see Fig. 1), that is, azimuthal periodicity of flow and temperature fields was assumed. Slight differences in generated heat in peripheral rods (less than 0.15 %) were neglected and maximum (22.52 kW in Case B1 and 34.13 kW in Case B2) were used for the peripheral rods.
- Heat fluxes on cladding inner surfaces (Table II) were determined from generated heat in Case B1 and Case B2 assuming homogeneous heat generation. Conjugated heat transfer was therefore assumed.

Table II. Inlet and wall boundary conditions

Case	Inlet flow rate [kg/s]	Wall heat flux central rod [kW/m^2]	Wall heat flux side rod [kW/m^2]
Case A1	0.03657	-	-
Case B1	0.02318	695.8	796.3
Case B2	0.022944	1 207.6	1 205.5

Computational domain is shown in Fig. 1 with basic mesh (Mesh A); spacers are modeled as honeycomb structures (thickness of 0.35 mm); vertical wires (diameter of 0.3 mm) were not modeled.

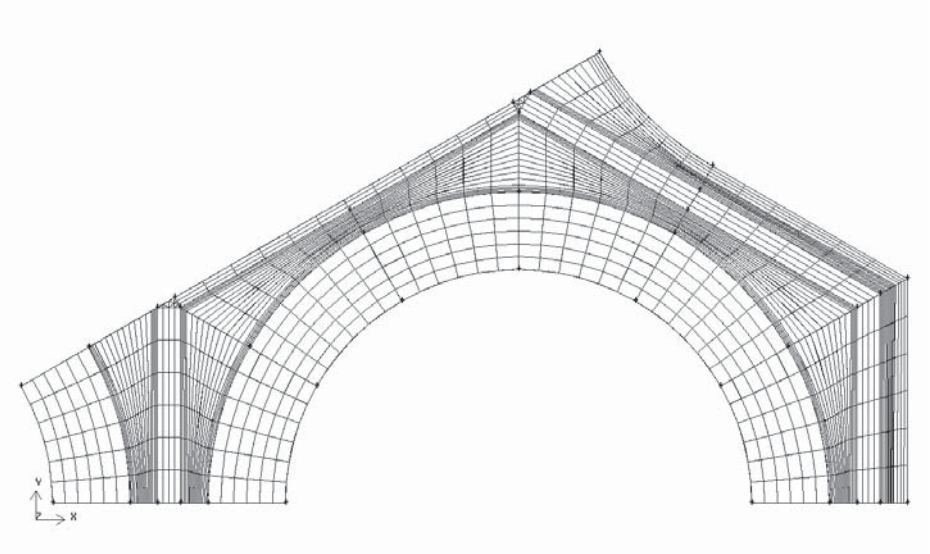

Fig. 1: Horizontal view of the basic mesh (labeled A)

Basic data on meshes used during "blind" phase of calculations are in Table III. Fine mesh is used on solid walls which is important mainly on heated walls. Azimuthal angle around each rod is measured from the direction of x-axis which corresponds to 90 degrees and increases counterclockwise. Therefore, gap region corresponds to 90 degrees for central rod and 270 degrees for peripheral rod.

Table III. Parameters of computational meshes

Mesh	A	B	C	D
First cell thickness [mm]	0.02	0.005	0.005	0.001
Number of rows of fine cells	4	6	6	8
Fine region total thickness [mm]	0.086	0.0386	0.0386	0.0114
Aspect ratio	283	708	618	773
Size change	4	12.5	12.5	52
Total cells, Cases B1, B2	1 387 100	1 977 260	4 045 220	5 645 360

Squish and equi-size skew were the same for all meshes (0.244 and 0.5, respectively).

SIMPLE algorithm was used for coupling of velocity and pressure fields. Computations were started with 1st order upwind discretization and after some decrease of scaled residuals, 2nd order upwind for momentum and QUICK discretization for energy was used. Decrease of scaled residuals of energy by eight orders, and of scaled residuals of the remaining variables by five orders was set as convergence limit.

Water properties were calculated by means of REFPROP 7 database available in the ANSYS FLUENT 12. Properties of Inconel 600 (cladding and spacers) were delivered by JAEA experimentalists. The values used in calculations are summarized in Table IV.

Calculations of Case B2 started from converged calculation of Case B1 and proceeded in several steps with increasing inlet temperature in order to avoid early failure of calculation due to water temperature exceeding the limit of REFPROP 7 tables.

Table IV. Properties of Inconel 600

Case	Density [kg/m^3]	Specific heat [J/kg/K]	Thermal conductivity [W/m/K]
Case B1	8250	475	16.5
Case B2	8290	500	19

4. RESULTS

4.1. Blind phase simulations

Simulations of the Case A1 were performed on meshes with solid zones (cladding, spacers) deleted. Pressure drop between axial positions z = 0.144 m and z = 1.340 m as measured from the start of heated section were determined as shown in Table V. The coarsest mesh (Mesh A) produced the best result which is quite frequent case ("compensation of errors").

Table V. Pressure drops (Case A1)

Mesh	Pressure drop [kPa]
A	64.0
B	68.0
C	69.0
D	69.2
Experiment	58.1

In Figs. 2 and 3, side rod wall temperatures for Case B1 at azimuthal angles of 240 degrees (position towards the center of the subchannel) and 270 degrees (position towards the subchannel gap) are shown. The meshes B and C produced almost identical results, the mesh D led to slightly higher temperatures. Character of all curves is similar.

Much larger differences between the three coarser meshes and the finest one can be seen in Figs. 4 and 5. The wall temperatures strongly depend on computational grid and there are large over-predictions in the case of grid D. Similar over-predictions were obtained also by authors of [4]. It must be repeated here, that all calculations presented in this paper are converged solutions within the same limits (decrease of scaled residuals by 8 orders for energy and by 5 orders for the other dependent variables). It is obvious, that the results on mesh D are not realistic. The mesh D differs mainly by the thickness of the near-wall cells, total thickness of the fine-mesh region, and the size change between neighboring cells (see Table III). The mesh worked without problems in simulations of case B1, but failed in simulations of Case B2. The sudden increase of wall temperatures is coincident with water temperature reaching the pseudo-critical temperature. Determination of cause of this behavior will be a subject of further studies.

Nevertheless it must be stated, that on all meshes used in the "blind" simulations, regions with heat transfer deterioration were seen in the Case B2.

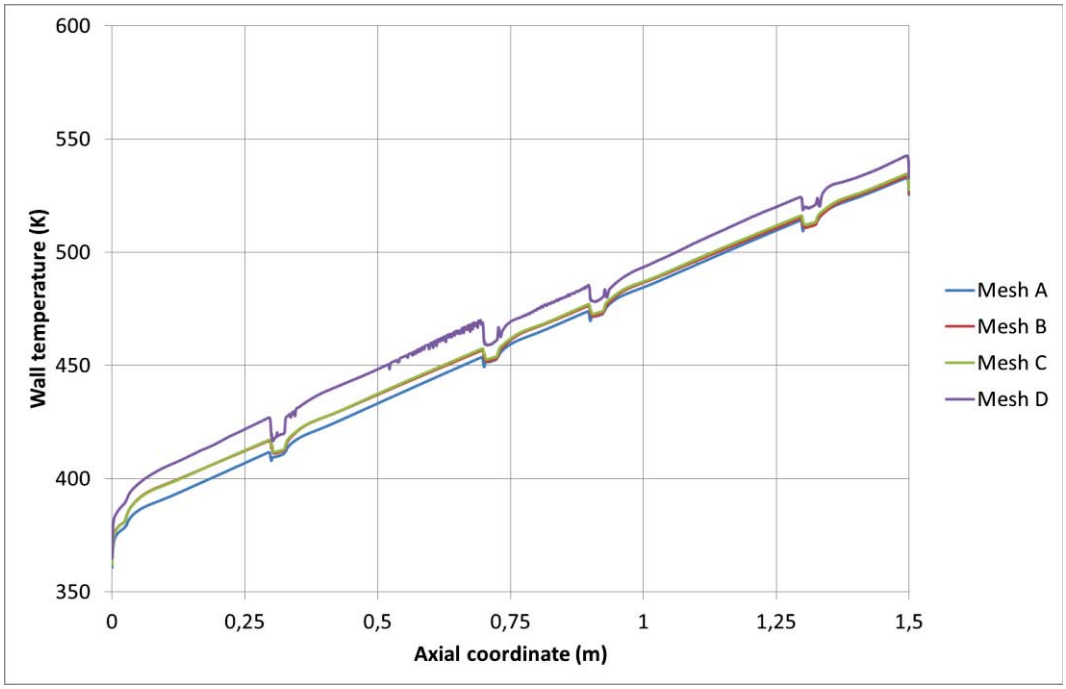

Fig. 2: Case B1 wall temperatures on side rod at 240 deg

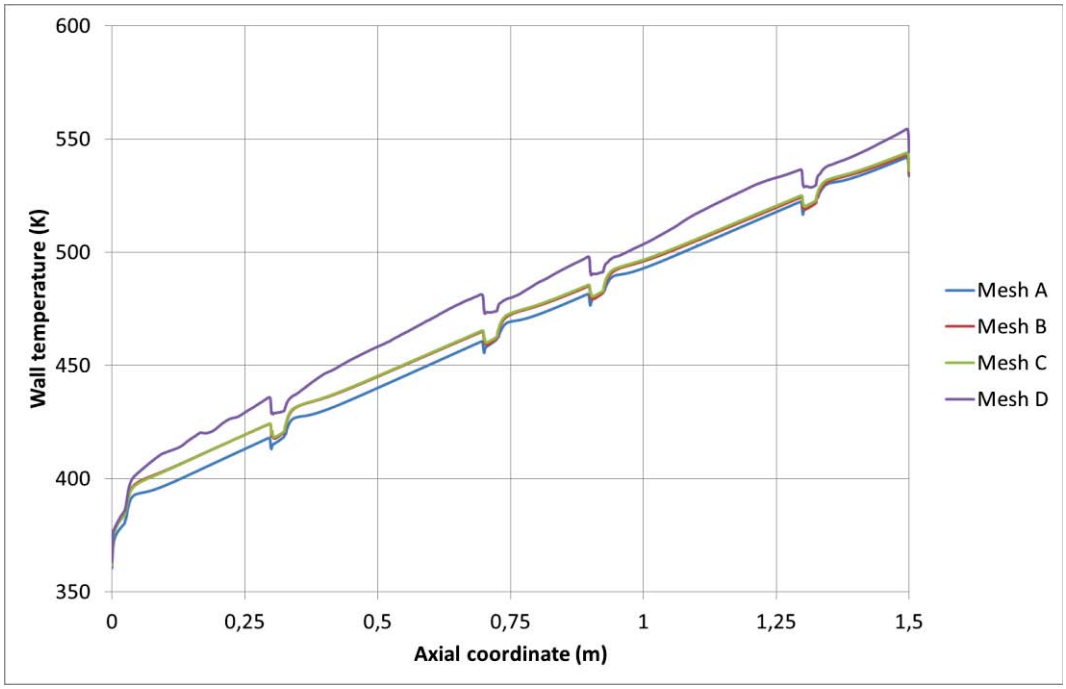

Fig. 3: Case B1 wall temperatures on side rod at 270 deg.

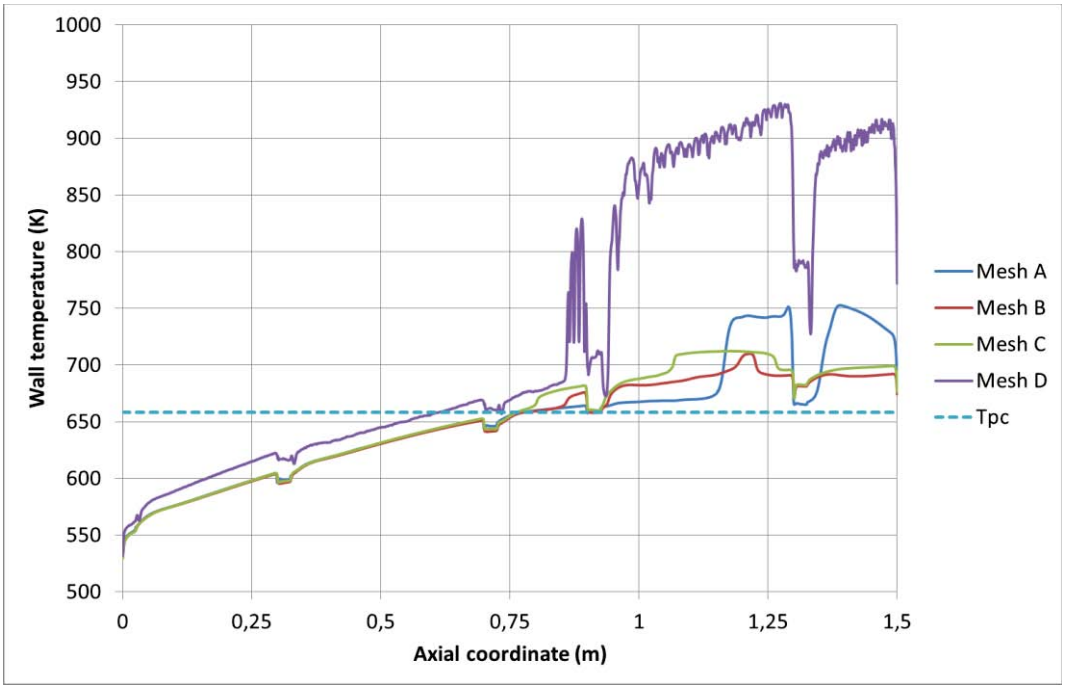

Fig. 4: Case B2 wall temperatures on side rod at 240 deg.

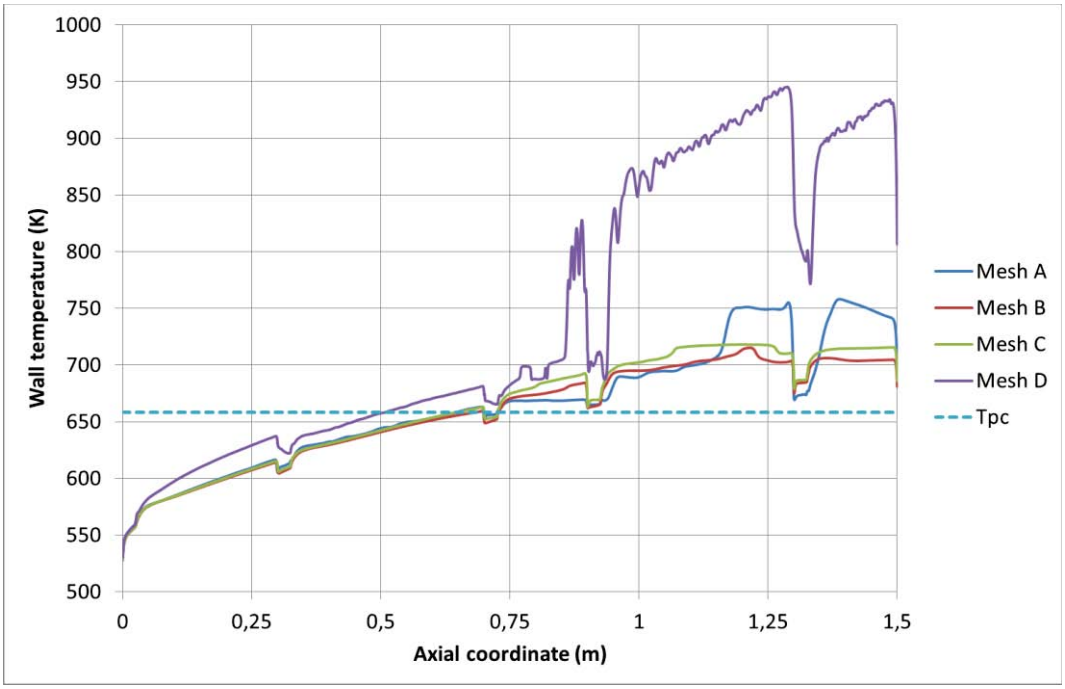

Fig. 5: Case B2 wall temperatures on side rod at 270 deg.

Comparison of "blind" results on mesh C with experimental data is shown in Figs. 6 and 7 for the Case B1 and in Figs. 8 and 9 for the Case B2. Here, data measured by thermocouples on all side rods at corresponding azimuthal positions (subchannel center and subchannel gap) were used in order to have

more experimental points for comparison. Again, this assumption of periodicity worked well in Case B1, but failed in Case B2 when regions with heat transfer deterioration appeared.

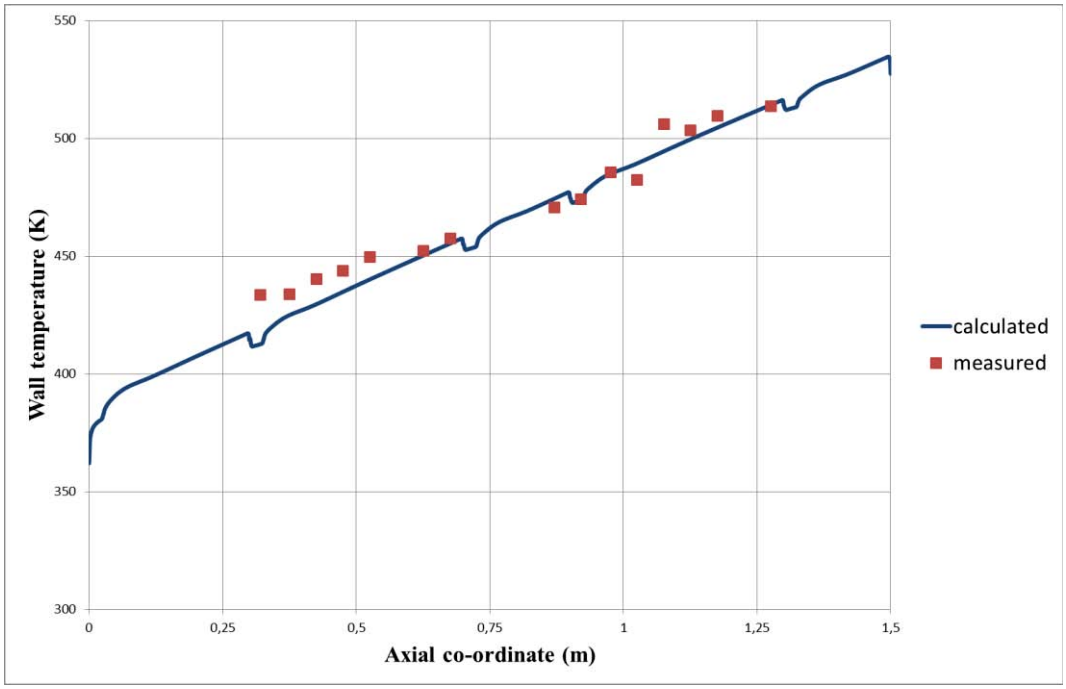

Fig. 6: Measured and computed side rod wall temperatures (Case B1, angle of 240 deg)

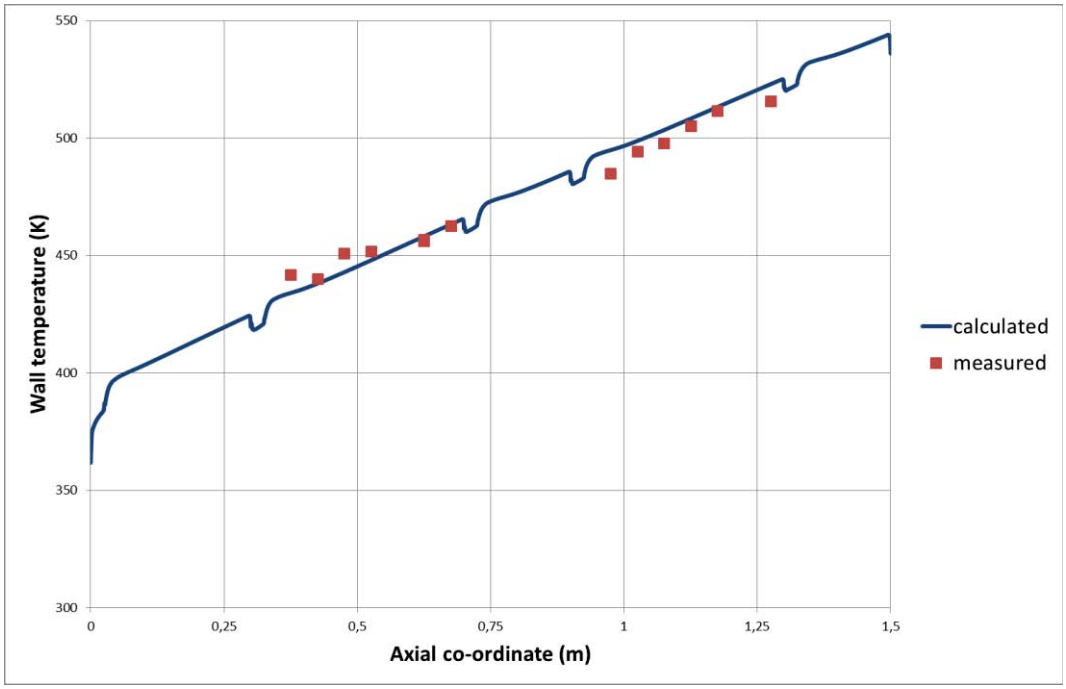

Fig. 7: Measured and computed side rod wall temperatures (Case B1, angle of 270 deg)

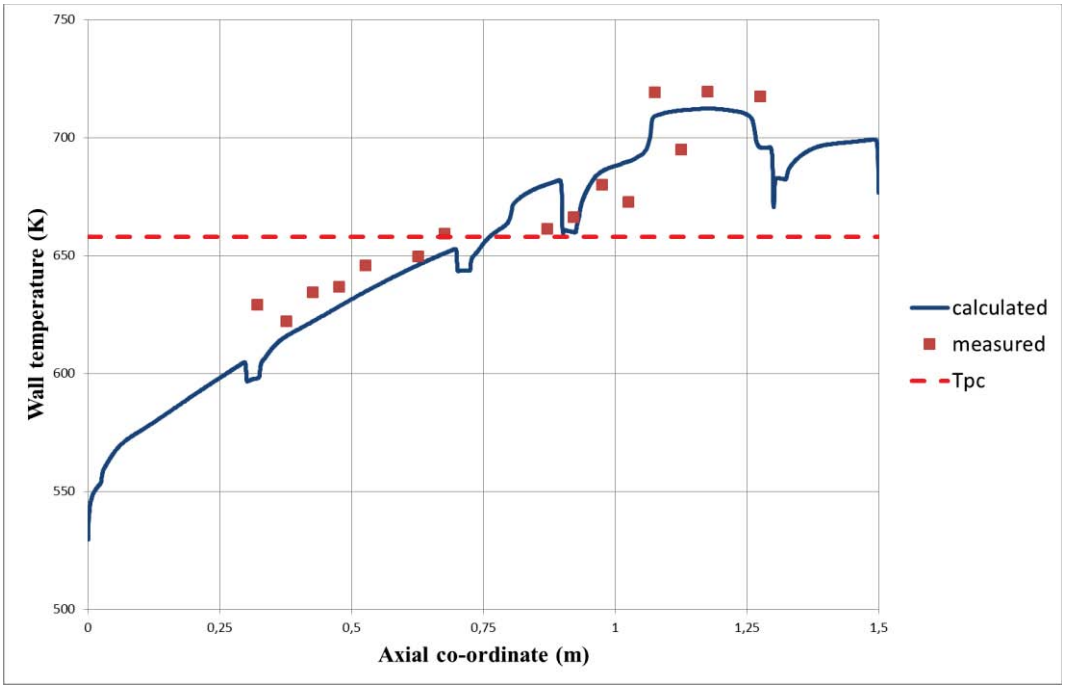

Fig. 8: Measured and computed side rod wall temperatures (Case B2, angle of 240 deg)

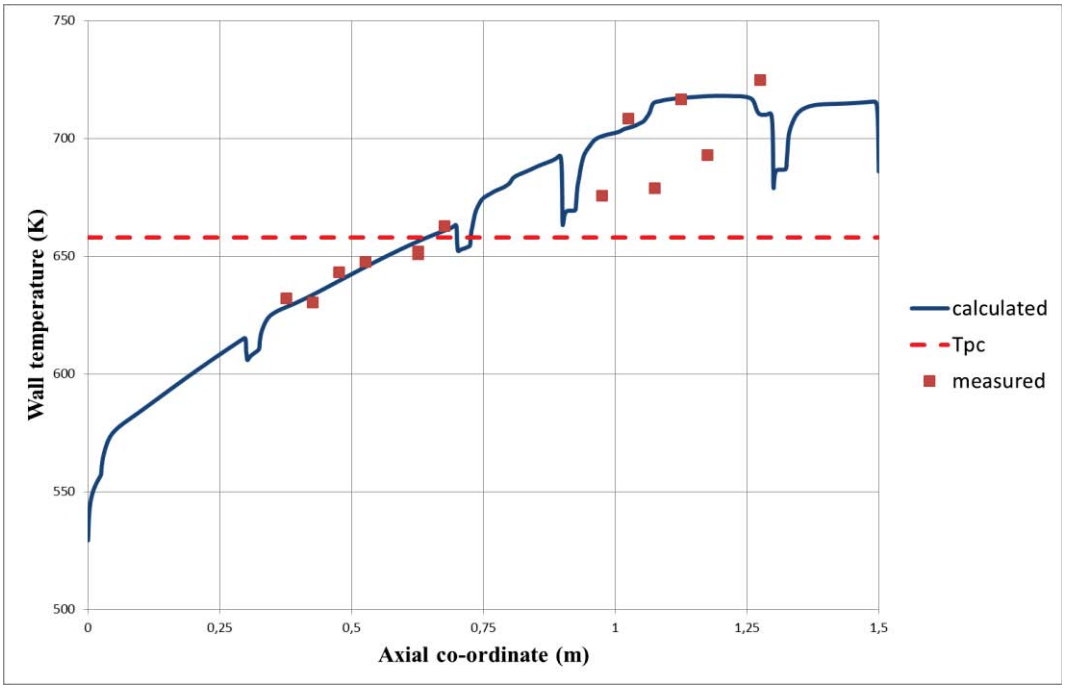

Fig. 9: Measured and computed side rod wall temperatures (Case B2, angle of 270 deg)

The comparisons indicate that the numerical approach adopted in this study could produce reasonable results and can be a basis of further development. However, some questions remain unanswered, still.

4.2. Aftermath simulations

Analysis of "blind" results showed that the mesh C produces results closest to experimental data. It can be therefore assumed that at least some physical phenomena taking place in the simulated experiments are resolved to some degree. During aftermath simulations, effect of spacers and buoyancy Case B2 were performed on this mesh. Resulting wall temperatures for azimuthal angles 240 degrees and 270 degrees are shown in Figs. 10 and 11. Experimental values are also shown for comparison.

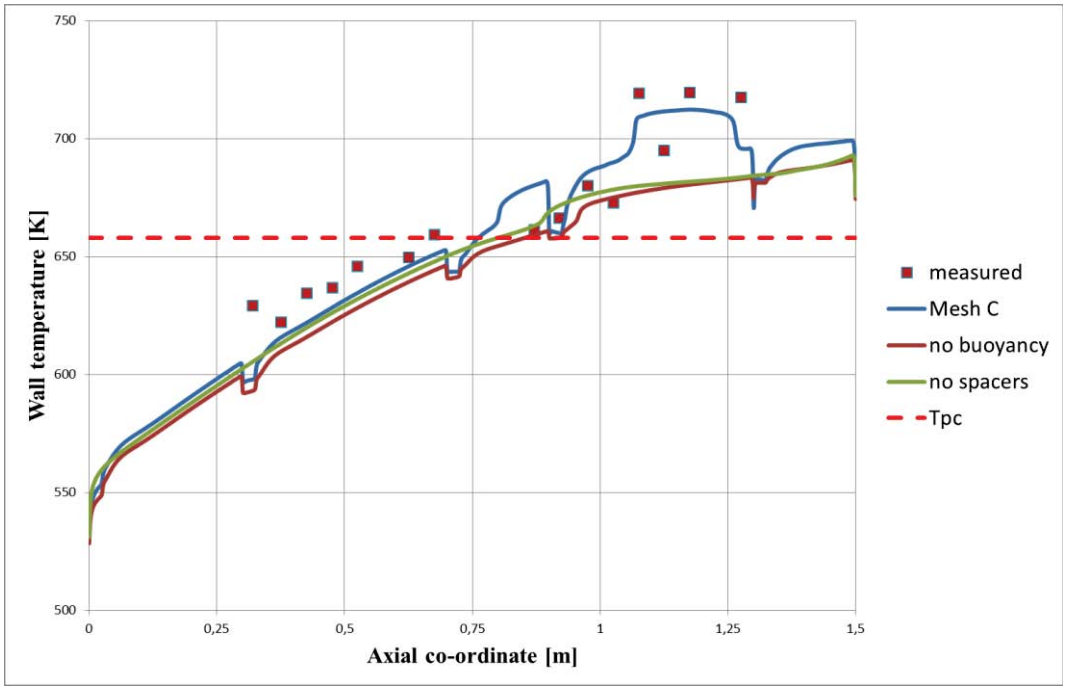

Fig. 10: Case B2, Mesh C, 240 deg

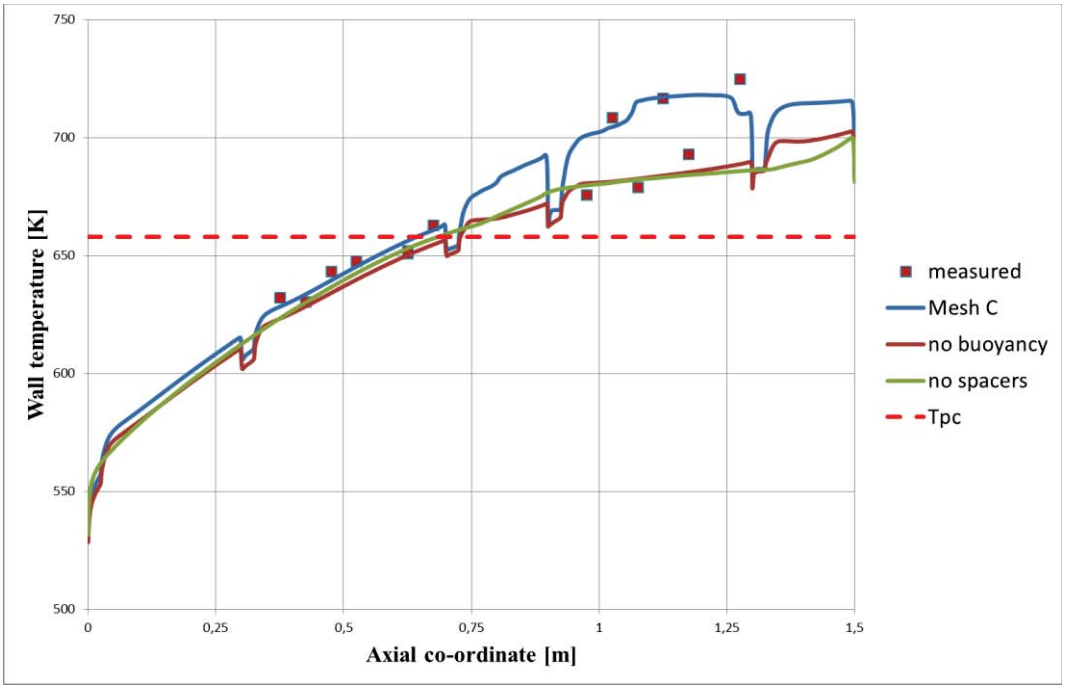

Fig. 11: Case B2, Mesh C, 270 deg

The Figs.10 and 11 indicate that spacers and buoyancy play very probably some role in onset of the heat transfer deterioration.

5. CONCLUSIONS

Benchmark calculations revealed that the k – ω SST model of turbulence in the ANSYS FLUENT 12 was able at least qualitatively to simulate heat transfer deterioration measured in the JAEA experiment.

It is probable that the flow and temperature fields do not follow the geometric symmetry of the rod bundle as assumed in the simulations. In the Case B2, the region of HTD appears dependent on azimuthal location and the shapes of axial course of the rod wall temperature suggest that different mechanisms of this phenomenon can be present there. It is also possible that the involved processes are unsteady after the near wall water temperature passes the pseudo-critical temperature.

The aftermath simulations indicate that presence of spacers can affect onset of the heat transfer deterioration. Also effect of buoyancy on this phenomenon can be seen in Figs. 10 and 11.

Computational meshes produced realistic results with the exception of the finest ones. One reason could be the large size change observed in this case and low overall thickness of the fine mesh layer. Ability of mesh to resolve the region with large changes of water properties can be important factor. Supplementing calculations are necessary in order to confirm or to discard this hypothesis.

REFERENCES

1. M. Rohde, J. W. R. Peeters, A. Pucciarelli, A. Kiss, Y. Rao, E. N. Onder, P. Mühlbauer, A. Batta, M. Hartig, V. Chatoorgoon, R. Thiele, D. Chang, S. Tavoularis, D. Novog, D. McClure, M. Gradecka, and K. Takase, “A Blind, Numerical Benchmark Study on Supercritical Water Heat Transfer

Experiments in a 7-Rod Bundle," *Proceedings of the 7th International Symposium on Supercritical Water/Cooled Reactors (ISSCWR-7),* Helsinki, Finland, March 15-18, 2015.

2. E. N. Pis'menny, V. G. Razumovskiy, E. M. Maevskiy, A. E. Koloskov, and I. L. Pioro, "Heat Transfer to Supercritical Water in Gaseous State or Affected by Mixed Convection in Vertical Tubes" *Proceedings of ICONE14 International Conference on Nuclear Engineering,* Miami, Florida, USA, July 17-20, 2006, Paper ICONE14-89483.

3. M. Jaromin, H. Anglart, "A numerical study of heat transfer to supercritical water flowing upward in vertical tubes under normal and deteriorated conditions," *Nucl. Eng. Des.* **264** (1), pp. 61-70 (2013).

4. M. Gradecka, R. Thiele, H. Anglart,"CFD Investigation of Supercritical Water Flow and Heat Transfer in a Rod Bundle with Grid Spacers," ," *Proceedings of the 7th International Symposium on Supercritical Water/Cooled Reactors (ISSCWR-7),* Helsinki, Finland, March 15-18, 2015.